

See discussions, stats, and author profiles for this publication at: <https://www.researchgate.net/publication/235795477>

Theoretical Study of the Decomposition of Formamide in the Presence of Water Molecules

ARTICLE in THE JOURNAL OF PHYSICAL CHEMISTRY A · MARCH 2013

Impact Factor: 2.69 · DOI: 10.1021/jp312853j · Source: PubMed

CITATIONS

17

READS

50

4 AUTHORS, INCLUDING:



Nguyen Vinh Son

University of Leuven

35 PUBLICATIONS 488 CITATIONS

SEE PROFILE



T. M. Orlando

Georgia Institute of Technology

197 PUBLICATIONS 2,737 CITATIONS

SEE PROFILE



Minh Tho Nguyen

University of Leuven

748 PUBLICATIONS 10,846 CITATIONS

SEE PROFILE

Theoretical Study of the Decomposition of Formamide in the Presence of Water Molecules

Vinh Son Nguyen,[†] Thomas M. Orlando,[‡] Jerzy Leszczynski,[§] and Minh Tho Nguyen^{*,†}

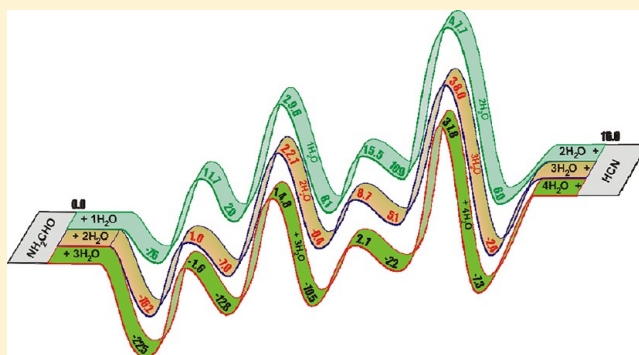
[†]Department of Chemistry, University of Leuven, B-3001 Leuven, Belgium

[‡]School of Chemistry and Biochemistry, Georgia Institute of Technology, Atlanta, Georgia 30332-0400, United States

[§]Interdisciplinary Center for Nanotoxicity, Department of Chemistry, Jackson State University, Jackson, Mississippi 39217-0510, United States

S Supporting Information

ABSTRACT: Formamide (NH_2CHO , FM) has been considered an active key precursor in prebiotic chemistry on early Earth. Under certain conditions such as dry lagoons, FM can decompose to produce reactants that lead to formation of more complex biomolecules. Specifically, FM decomposition follows many reactive channels producing small molecules such as H_2 , CO , H_2O , HCN , HNC , NH_3 , and HNCO with comparable energy barriers in the range of 73–82 kcal/mol. Due to the likely presence of water on prebiotic Earth and the intrinsic presence of water following FM decomposition, we explore the effects of water oligomers, $(\text{H}_2\text{O})_n$ with $n = 1–3$, on its dehydration, dehydrogenation, and decarbonylation reactions using quantum chemical computations. Geometries are optimized using MP2/aug-cc-pVxZ calculations ($x = \text{D}, \text{T}$), and relative energies are evaluated using coupled-cluster theory CCSD(T) with the aug-cc-pVxZ basis sets ($x = \text{D}, \text{T}, \text{Q}$). Where possible the coupled-cluster energies are extrapolated to the complete basis set limit (CBS). Water classically acts as an efficient bifunctional catalyst for decomposition. With the presence of one water molecule, the dehydration pathway leading to HCN is favored. When two and three water molecules are involved, dehydration remains energetically favored over other channels and attains an energy barrier of ~ 30 kcal/mol.



1. INTRODUCTION

An essential issue in prebiotic chemistry of early Earth and its atmosphere concerns the role and presence of simple molecules in formation of more complex molecular systems. The potential of HCN chemistry in a prebiotic perspective has been the focus of several decades of studies,^{1–15} as highlighted by the seminal synthesis of adenine reported earlier by Oro^{13,14} as a product of cyanide hydrogen polymerization. Moreover, in the interstellar media, HCN and H_2O are both the most abundant three-atom organic compounds. Molecules in the interstellar media that are made of the four biologically relevant and common elements H, C, N, and O include isocyanic acid (HNCO) and formamide (NH_2HCO , denoted hereafter as FM).^{1–7} While the former is not stable, the latter is a stable organic compound produced from the HCN hydrolysis reaction. Its presence was indeed detected in the gas-phase interstellar media,⁸ in the long-period comet Hale–Bopp,⁹ and tentatively also in the solid phase on grains around the young stellar object W33A,¹⁰ as well as in the protostellar source NGC 7538 IRS9.¹¹ On the basis of the FM high boiling point, it also can be present and somewhat concentrated in drying lagoons.

In this paper, we further address whether FM initially decomposes into smaller species or acts directly as a biomolecular precursor. Previously, we carried out a theoretical

study¹⁶ on the thermal decomposition pathways of FM using a combination of electronic structure computations and kinetic RRKM rate theory analysis. Calculated results predicted that dehydration of FM yielding $\text{H}_2\text{O} + \text{HCN}$ is the most favorable route, but the corresponding energy barrier of >70 kcal/mol is too high for a gaseous-phase reaction without interaction with third bodies. Many studies by Saladino and DiMauro¹⁵ and more recently by Springsteen and co-workers¹⁷ reported the synthesis of adenine and purine upon heating a solution of neat formamide up to 150–180 °C. Springsteen and co-workers¹⁷ were able to identify a few intermediates such as 2-iminoacetonitrile, which is a formal dimer of HCN and a strong electrophile for formation of either purine or adenine. They proposed a mechanism which begins with dehydration of formamide to hydrogen cyanide. The influence of temperature and medium is thus clearly important.

In the last decades, a large number of studies^{18–33} have already been devoted to the interactions of FM with water through hydrogen bonds, and the systems investigated include several neighboring H_2O molecules. Both theoretical and experimental studies on the stabilities of the H-bonded complexes of

Received: December 30, 2012

Revised: March 4, 2013

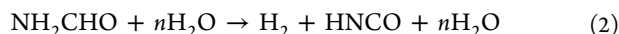
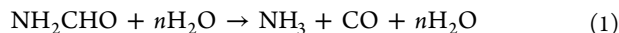
Published: March 5, 2013



formamide with water oligomers, $\text{FM}-(\text{H}_2\text{O})_n$ ($n = 1-8$) are indeed available.^{20,21,27,29,31,33} In recent papers, Sastry and co-workers^{34,35} investigated formation of hydrogen-bonded clusters of formamide clusters $[\text{HCONH}_2]_n$ ($n = 1-10$) and acetamide clusters $[\text{CH}_3\text{CONH}_2]_n$ ($n = 1-15$). Different kinds of linear, circular, helical, and stacked forms of formamide clusters, and linear, circular, standard, and crystal forms of acetamide clusters have been investigated using DFT theory. These studies pointed out that the cooperativity in hydrogen-bonded clusters could contribute to the effects observed in our study upon increasing size of the investigated water shell. Nevertheless, as the number of water molecules considered in the present work is rather small (up to 3), the inherent cooperative effect is expected to be small and could mutually be canceled when evaluating relative energies between stationary points.

Other studies mainly focused on the proton transfer processes of FM and its protonated form with the assisting-water molecules.^{22,24,26} The mechanisms of FM and its protonated/ionized forms reacting with water molecules leading to CO , NH_3 , and HCOOH were also investigated.^{19,23,25,27,32} In this context the role of the FM dimers and water molecules could be of crucial importance. However, to the best of our knowledge, a comprehensive investigation of the molecular mechanisms considering all possible decomposition processes of FM with water assistance is not available yet.

In relation to our recent theoretical study of formamide decomposition,¹⁶ we set out to carry out a theoretical study of the most important channels of FM decomposition with participation of water molecules $(\text{H}_2\text{O})_n$ using ab initio electronic structure theory calculations. The FM monomer decomposition channels studied included the decarbonylation (eq 1), dehydrogenation (eq 2), and dehydration (eq 3) pathways.



It is well known that when exerting its catalytic effect, water often does not involve a single molecule but rather a small oligomer.³⁶ Accordingly, a pertinent question is how many water molecules effectively take part in these chemical transformations through direct participation in the supermolecules rather than by microsolvation. For example, the actual number of active water molecules taking part in the hydration of carbon dioxide remains a matter of debate.^{37,38} The main objective of the present theoretical work is thus to probe the energetics and mechanisms of these gas-phase reactions without and with direct assistance of water oligomers.

The discussion hereunder begins with a summary of FM decomposition channels and products. The subsequent and main part of the paper describes the results with participation of one water molecule ($n = 1$) on different decomposition channels. The following section is concerned with FM dehydration with the presence of two and three water molecules ($n = 2$ and 3). Finally, analysis of the topology of the electron densities of some representative transition structures is also presented.

It should be stressed that we are not addressing in this study the hydrolysis of FM, which is an important channel, and what is observed experimentally. We are rather concerned with the reverse hydrolysis reaction of FM, which likely occurs when the system is heated (thermal process at high temperature) or irradiated with photons (photostimulated processes).

2. COMPUTATIONAL METHODS

Electronic structure calculations were carried out using different levels of molecular orbital theory with the aid of the Gaussian 03³⁹ and Molpro⁴⁰ programs. Initial geometry optimizations were first performed using second-order Møller–Plesset perturbation theory (MP2) with the correlation-consistent aug-cc-pVDZ basis set. Harmonic vibrational frequencies were evaluated at this level to characterize the stationary structures located. Geometrical parameters of the relevant equilibrium and transition (TS) structures were then reoptimized using the MP2 method but with the larger aug-cc-pVTZ basis set. In order to obtain improved relative energies, single-point electronic energies were subsequently obtained by extrapolating the coupled-cluster theory CCSD(T)^{41,42} energies in conjunction with the correlation-consistent aug-cc-pVxZ ($x = \text{D, T, and Q}$) basis sets^{43,44} to the complete basis set (CBS) limit, based on MP2/aug-cc-pVTZ-optimized geometries. For simplicity, correlation-consistent basis sets are denoted hereafter as aVxZ. For some open-shell species, the fully unrestricted formalism (UHF, UMP2) is used with Gaussian 03. The CCSD(T) energies are extrapolated to the complete basis set (CBS) limit energies using expression 4.⁴⁵

$$E(x) = A_{\text{CBS}} + B \exp[-(x-1)] + C \exp[-(x-1)^2] \quad (4)$$

Although one can extrapolate the HF and correlation energies separately, this does not substantially improve the fits. The relative energies between stationary points on the different pathways are then obtained from CCSD(T)/CBS total energies and corrected for the zero-point vibrational energy (ZPE) contributions. ZPE values are obtained from MP2/aVDZ harmonic vibrational frequencies. For the system with $n = 3$ where the CBS extrapolation is not possible, due to a limitation of our computational resources, relative energies are determined at the CCSD(T)/aVTZ + ZPE level.

3. RESULTS AND DISCUSSION

As for a convention, each structure considered in the following sections is labeled by a combination of letters and numbers, in which the letters **ts** or **TS** stand for a transition structure connecting two equilibrium structures. In most cases, the identity of a TS can easily be determined. In some more ambiguous cases, intrinsic reaction coordinates (IRC) calculations are carried out to establish the connection of a TS with two local minima.

3.1. Summary of Formamide Unimolecular Decomposition (without water, $n = 0$). In our previous study,¹⁶ decomposition of FM was investigated in detail using similar electronic structure computations at the CCSD(T)/CBS level. Let us first briefly summarize the main results related to FM fragmentation and thus formation of small molecules including H_2 , CO , H_2O , HCN , HNC , NH_3 , and HNCO . These species were produced in processes having comparable energy barriers in the range of 73–82 kcal/mol. Figure 1 shows the possible reaction channels and products of the FM unimolecular decomposition. The H_2 -loss channel is favored in a one-step process, although the two-step counterpart (not shown) is competitive. For CO elimination, the two-step channel involving the carbene $\text{NH}_2\text{—C—OH}$ intermediate is clearly more favorable than the one-step channel and also more favorable than the one-step H_2 loss.

Accordingly, HCN formation from FM is basically a multistep process passing through a formimidic acid isomer, which

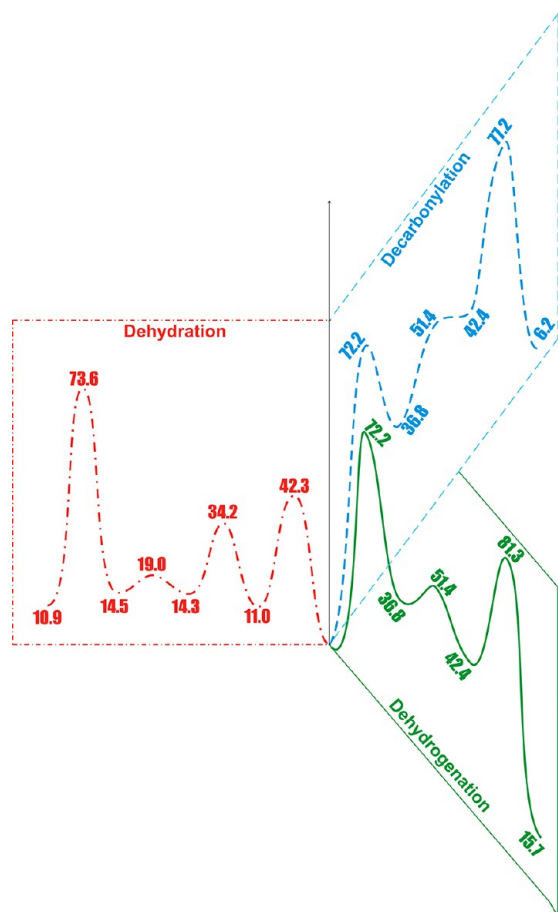


Figure 1. Possible reaction channels of the unimolecular decomposition of formamide including dehydration, decarbonylation, and dehydrogenation. Corresponding energy barriers are obtained using CCSD(T)/CBS + ZPE calculations (kcal/mol).

subsequently undergoes a rate-determining dehydration (Figure 1). Indeed, the rate of multistep decomposition yielding $\text{H}_2\text{O} + \text{HCN}$ was found to be the fastest kinetic rate with the lowest energy barrier (73 kcal/mol) and largest pre-exponential factor ($5.69 \times 10^{13} \text{ s}^{-1}$) over a large range of temperature and pressure.¹⁶ This finding suggests that the water molecules formed in such a way can in turn act as a catalyst for the subsequent fragmentation processes of FM. In other words, there is an intrinsic water-mediated decomposition of FM that could occur in a medium without pre-existing water. In the next sections, we explore in some detail the catalytic effects of water molecules on its decarbonylation, dehydrogenation, and dehydration.

As for a necessary calibration for the calculated MO results obtained in this work, Table 1 lists a comprehensive comparison of the variations of relative energies with respect to the one-electron basis functions. CCSD(T) relative energies are calculated with the correlation-consistent aVxZ basis sets and their CBS extrapolations. Again, it is confirmed that the CCSD(T)/aVTZ relative values differ by around ± 1.0 kcal/mol from the best estimates at the CCSD(T)/CBS-aVxZ level. Therefore, in constructing the potential energy surfaces of the larger systems, the CCSD(T)/aVTZ + ZPE level can be employed to obtain reliable theoretical estimates for relative energies between stationary structures.

3.2. Effect of One Water Molecule on FM Decomposition ($n = 1$). We first relocate the lowest lying H-bonded complexes between formamide and water. These complexes have been the subject of extensive experimental and theoretical studies in the past several decades (cf. for instance refs 18–32). It is not the purpose of the present study to reinvestigate them further. They constitute in our present purpose the initial preassociation complexes for subsequent transformations. Figure 2 summarizes the shape, selected geometrical parameters, and complexation energies of the three lowest lying H-bonded complexes which are labeled as **W1-FM**, **W2-FM**, and **W3-FM**. For the purpose of abbreviation, the letter **W** denotes a water molecule whereas the number **X**, ranging from 1 to 3, stands for a decreasing ordering of stability. Our present results agree well with numerous previous reports on the FM–water complexes (cf. refs 18–32).

According to complexation energies (Figure 2), **W1-FM** is the most stable H-bonded complex which is located at 7.4 kcal/mol below the separated $\text{NH}_2\text{CHO} + \text{H}_2\text{O}$ monomers. **W2-FM** and **W3-FM** have smaller binding energies of 4.9 and 3.9 kcal/mol, respectively. **W1-FM** and **W2-FM** each has two O–H hydrogen bonds which are formed by two kinds of interactions. In **W1-FM**, two hydrogen bonds are formed by $\text{H}_\text{N} \cdots \text{O}_\text{W}$ and $\text{H}_\text{W} \cdots \text{O}_\text{FM}$ interactions, while $\text{H}_\text{C} \cdots \text{O}_\text{W}$ and $\text{H}_\text{W} \cdots \text{O}_\text{FM}$ hydrogen bonds are constructed in **W2-FM**. Even though **W1-FM** and **W2-FM** have the same kind of $\text{OH} \cdots \text{O}$ interaction, their bond distances are not similar. The $\text{OH} \cdots \text{O}$ bond distance in **W1-FM** amounts to 1.875 Å, which is 0.014 Å shorter than **W2-FM**. The distances of other hydrogen bonds are significantly longer, namely, 2.036 Å for $\text{H}_\text{N} \cdots \text{O}_\text{W}$ in **W1-FM** and 2.636 Å for $\text{H}_\text{C} \cdots \text{O}_\text{W}$ in **W2-FM**. The nature of the H-bond donors, OH, NH, and CH, is clearly reflected in the relative stability of both complexes. **W3-FM** has only one hydrogen bond which is formed by interaction of the O_W atom with the $\text{H}_\text{N}(\text{FM})$ atom (cf. Figure 2) and is therefore much less stable.

These well-known results point out that there are different ways for a water molecule of inducing significant stabilization through hydrogen bonding with FM (Figure 2). It can be expected that a FM stationary point, irrespective of its identity (equilibrium or transition structure), is more or less stabilized following H-bonded complexation with water. Table 2 summarizes such effects along a portion of the energy profile for FM decomposition in which a comparison between three types of interactions **W1**, **W2**, and **W3** is possible.

In fact, all of the complexed stationary points in **WX-FM** are stabilized as compared to the uncomplexed FM counterparts. With respect to the isolated monomeric reference, all complexed structures are lower on the energy scale (see ΔE values in Table 2), even though the resulting stabilization energies ΔE_stab are, as expected, not uniform. ΔE_stab is simply defined as the difference between the corresponding relative energies in the water-complexed **WX-FM** and free FM structures. Thus, ΔE_stab ranges from a value as small as -2.4 kcal/mol for **W3-INT1a** to as large as -31.3 kcal/mol for **W1-FM-TS143** (cf. value in Table 2, the structure of the latter is shown in a following section, Figure 5).

While most stationary points are stabilized from 3 to 8 kcal/mol, the two TSs for a 1,3-H shift giving an isomer (structures **tsH-1,3** in FM to **W1-FM-TS143**) and H_2O loss yielding HNC (structure **INT-2a-tsH₂O** in FM to **W1-FM-TSHNC**) are strongly stabilized by 31.3 and 19.8 kcal/mol, respectively.

These results point out the existence of two distinct categories of effects upon water interaction. While the first category arises mainly from the H-bonded microsolvation, the second is due to a

Table 1. Relative Energies (kcal/mol) of Some Reactants, TS, and Products of the $[\text{CH}_3\text{NO}]$ Energy Surface Obtained Using CCSD(T) with Different aug-cc-pVxZ Basis Sets ($x = \text{D, T, Q}$) and Extrapolated Complete Basis Set (CBS)^a

Structure	Geometry	aVDZ	aVTZ	aVQZ	CBS
NH₂CHO		0.0	0.0	0.0	0.0
H₂-ts1		78.0	78.5	78.7	78.8
INT-1c-tsH₂O		71.4	72.4	73.2	73.6
INT-1b-tsH₂O		79.9	81.6	82.3	82.7
INT-2b-tsNH₃		74.3	75.8	76.6	77.2
NH₃-ts		77.6	79.4	80.1	80.5
H₂ + HNCO		16.7	15.6	15.6	15.7
HCN + H₂O		14.3	16.0	16.5	16.9
NH₃ + CO		2.5	5.2	5.8	6.2

^aOptimized geometries at MP2/aVTZ. Relative energies are corrected for ZPE obtained from MP2/aVDZ harmonic vibrational frequencies.

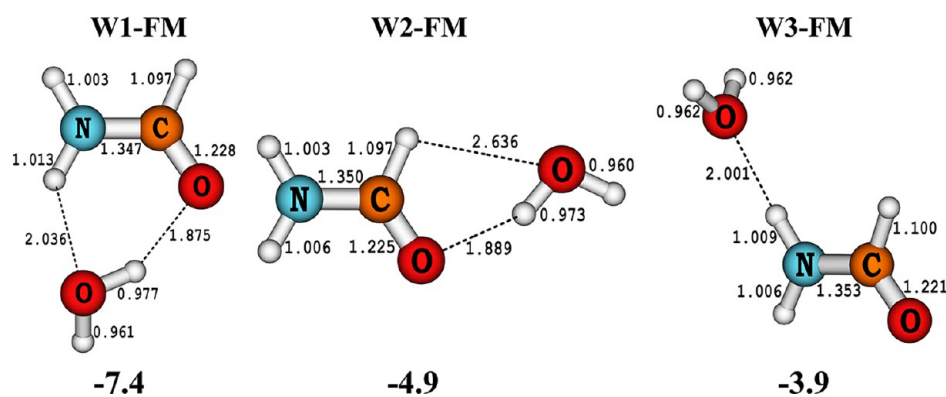


Figure 2. Three lower energy hydrogen-bonded complexes of formamide and water. Complexation energies (in kcal/mol) are obtained from CCSD(T)/CBS + ZPE computations.

Table 2. Stabilizing Effects of One Water Molecule on the Relative Energies of Stationary Points along the Profile of Formamide Decomposition^a

FM stationary structure	without water	with H-bonded interaction with one water molecule ^b		
		ΔE W1-xx ^c	ΔE W2-xx ^c	ΔE W3-xx ^c
NH ₂ CHO	0.0	−7.4 FM	−4.9 FM	−3.9 FM
INT-1a	11.0	2.5 FIA1a	8.1 FIA1a	8.6
INT-1b	14.3	8.5 FIA1b	11.9 FIA1b	9.6
INT-1c	14.5	11.6 FIA1c	8.7 FIA1c	9.3
INT-2a	36.8	32.3 AHCt	29.1 AHCt	30.3
tsH-1,2	72.2	66.0 FM-TS12	68.7 FM-TSH12	68.2
tsH-1,3	43.9	12.6 FMTS-143	39.5 FM-TSH13	40.8
tsR-1a1b	34.0	29.9 FIA-TSAb	31.3 FIA-TSAb	30.2
tsR-1b1c	19.7	16.3 FIA-TSbc	17.0 FIA-TSbc	15.1
INT-1b-tsH ₂ O	82.7	80.5	77.4	
INT-1c-tsH ₂ O	73.6	68.8	69.0 FIA1c-TSHCN	69.8
INT-2a-tsH ₂ O	83.7	63.9 AHCt-TSHNC	77.1 FIA1a-TSHNC	78.8

^aRelative energies given in kcal/mol are obtained from CCSD(T)/CBS + ZPE. ^b ΔE are relative energies with respect to the separated reactants [NH₂CHO + H₂O]. ^cWn-xxx, n = 1, 2, and 3, are the labels of the corresponding structures given in Figures 2–5.

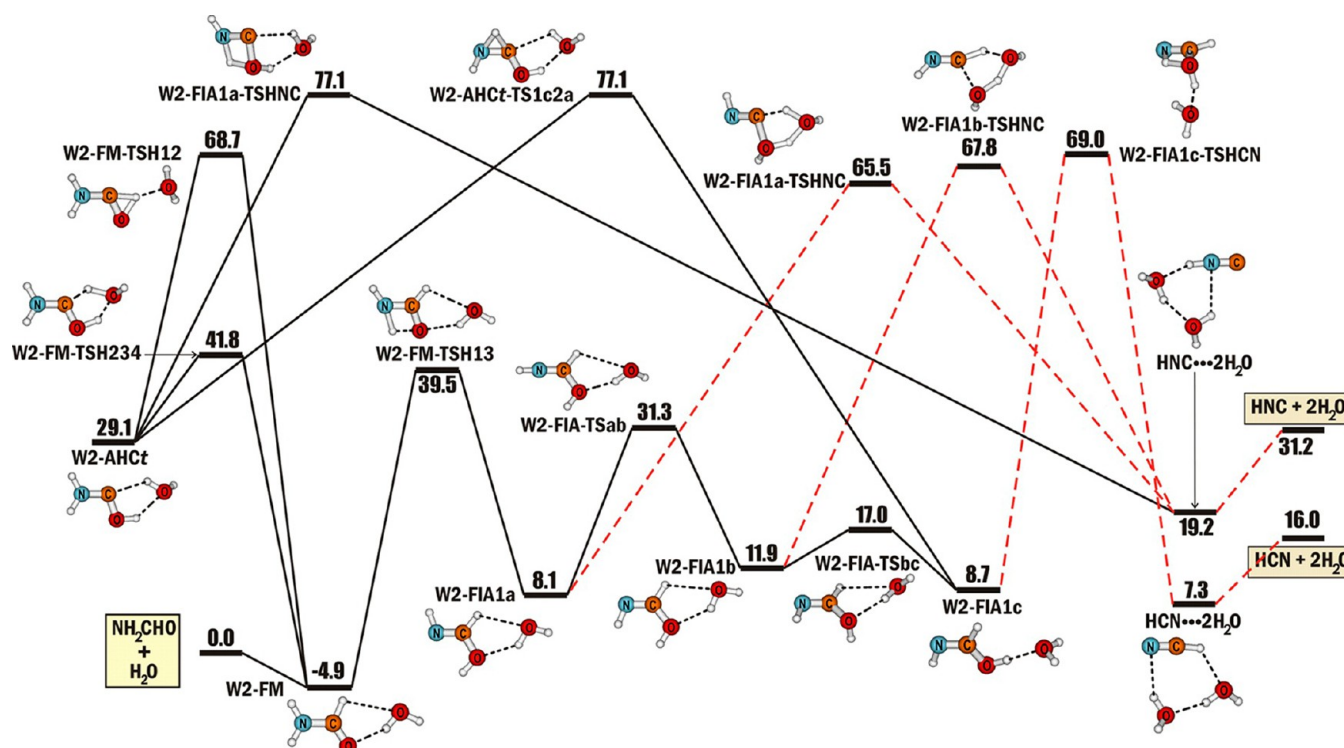


Figure 3. Dehydration pathways from complex W2-FM. Relative energies in kcal/mol are obtained from CCSD(T)/CBS + ZPE computations.

bifunctional catalytic effect. Both stabilizing effects are thus present in each type of WX interaction.

Let us first examine the pathways starting from the two less stable complexes. It appears that most, but not all, structures shown in Table 2 involving the W2-FM and W3-FM types of interaction belong to the first category. The stabilization energies ΔE_{stab} in both series are quite similar to each other ranging from 3 to 8 kcal/mol. This corresponds to the expected values for electrostatic H-bonded attractions. There is no substantial difference in ΔE_{stab} involving either an equilibrium structure (7.7 kcal/mol for W2-AHCt) or a transition state (4.7 kcal/mol for W2-FIA1c-TSHCN). Overall, the relative energy ordering in both cases remains unchanged with respect to the free unimolecular FM system. Due to the strong similarity between both W2 and W3 types of interaction, we consider the W2 series

in more detail. Some relevant pathways involving W3-FM structures will however be described.

The corresponding energy profiles that schematically illustrate the reaction pathways with the presence of one water molecule for dehydration are displayed in Figure 3 for the W2 type and Figure 4 for the W1 type. While Figure 5 shows dehydrogenation of both W1 and W2 types, Figure 6 summarizes decarbonylation in both W1 and W3 series. Shapes of some typical structures are depicted in Figure 7.

3.2.1. Energy Ordering between Complexed Isomers. FM has a number of low-energy isomers, including formaldimine (HN=CHOH) and aminohydroxy-carbene (H₂NCOH). These isomers also form H-bonded complexes with water. The formamide–water complex remains the lowest energy point in each series. The relative energy ordering between isomers

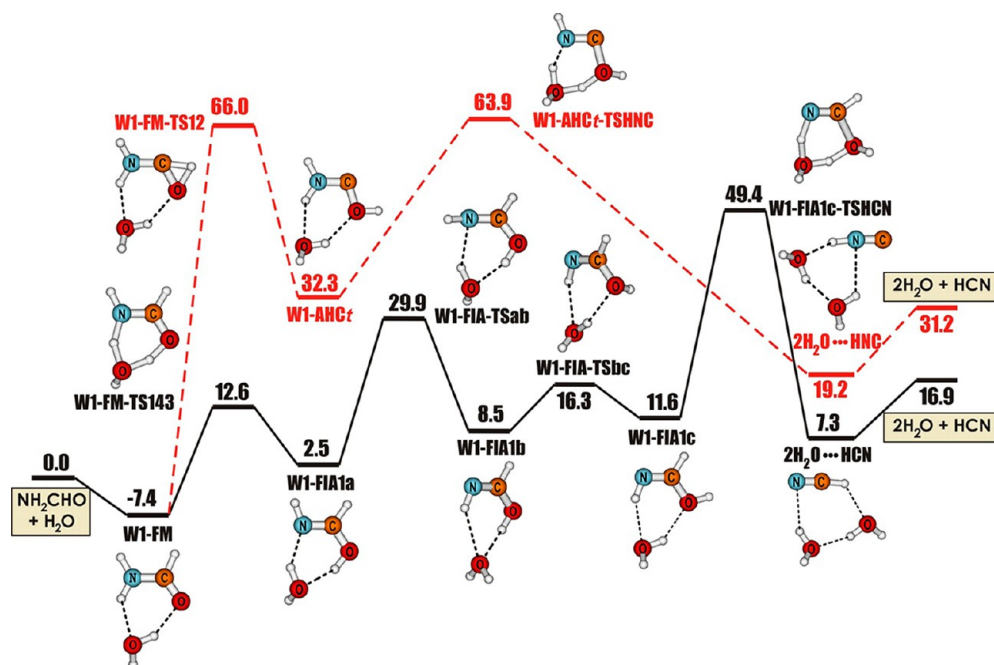


Figure 4. Dehydration pathways from complex W1-FM. Relative energies in kcal/mol are obtained from CCSD(T)/CBS + ZPE computations.

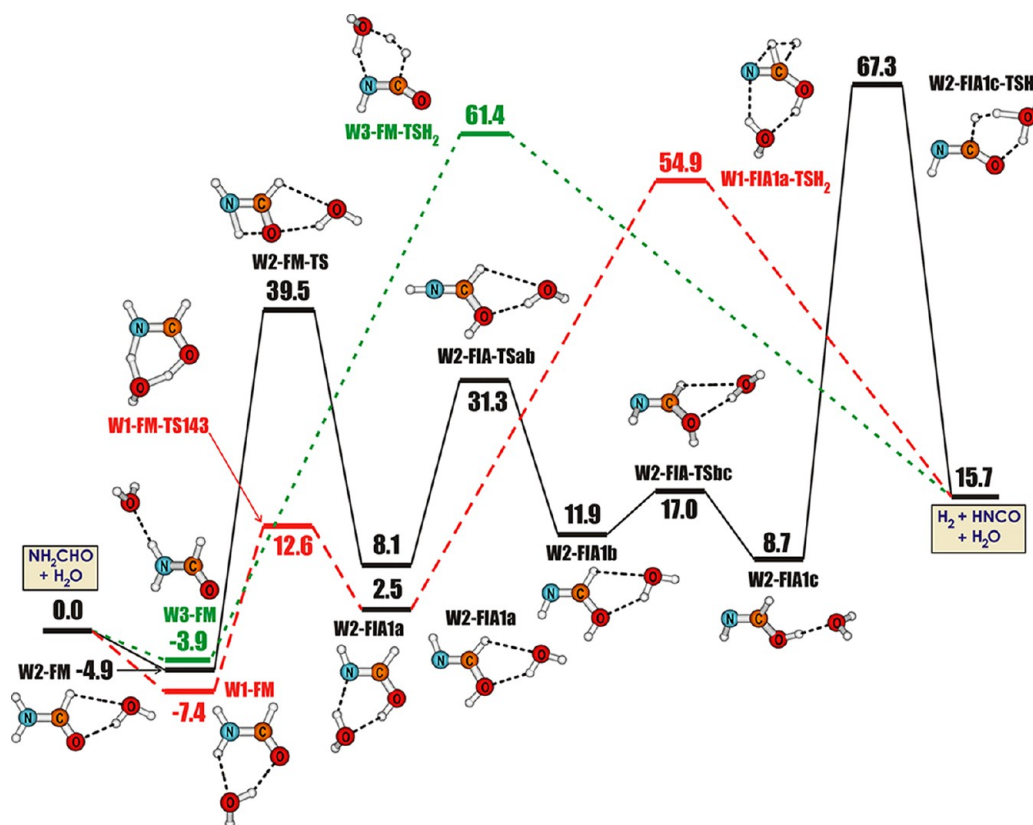


Figure 5. Dehydrogenation pathways from complexes W1-FM, W2-FM, and W3-FM. Relative energies in kcal/mol are obtained from CCSD(T)/CBS + ZPE computations.

remains unchanged in which formaldimine is less stable than FM but more stable than aminohydroxy-carbene.

Within the W2 type, conversion of W2-FM to the imine W2-FIA1a via the TS for 1,3-H-shift W2-FM-TSH13 (located at 39.5 kcal/mol) remains more favored than that of FM to the carbene W2-AHCt via W2-FM-TSH234 (at 41.8 kcal/mol, Figure 3).

With respect to unimolecular FM energetics illustrated in Figure 1, the FM-carbene interconversion is greatly facilitated by a water-assisted H transfer. Both TSs W2-FM-TSH12 and W2-FM-TSH234 illustrate well the intrinsic characteristics of the two categories of water interaction (Figure 3). While the former (located at 68.7 kcal/mol) corresponds to a H-bonded

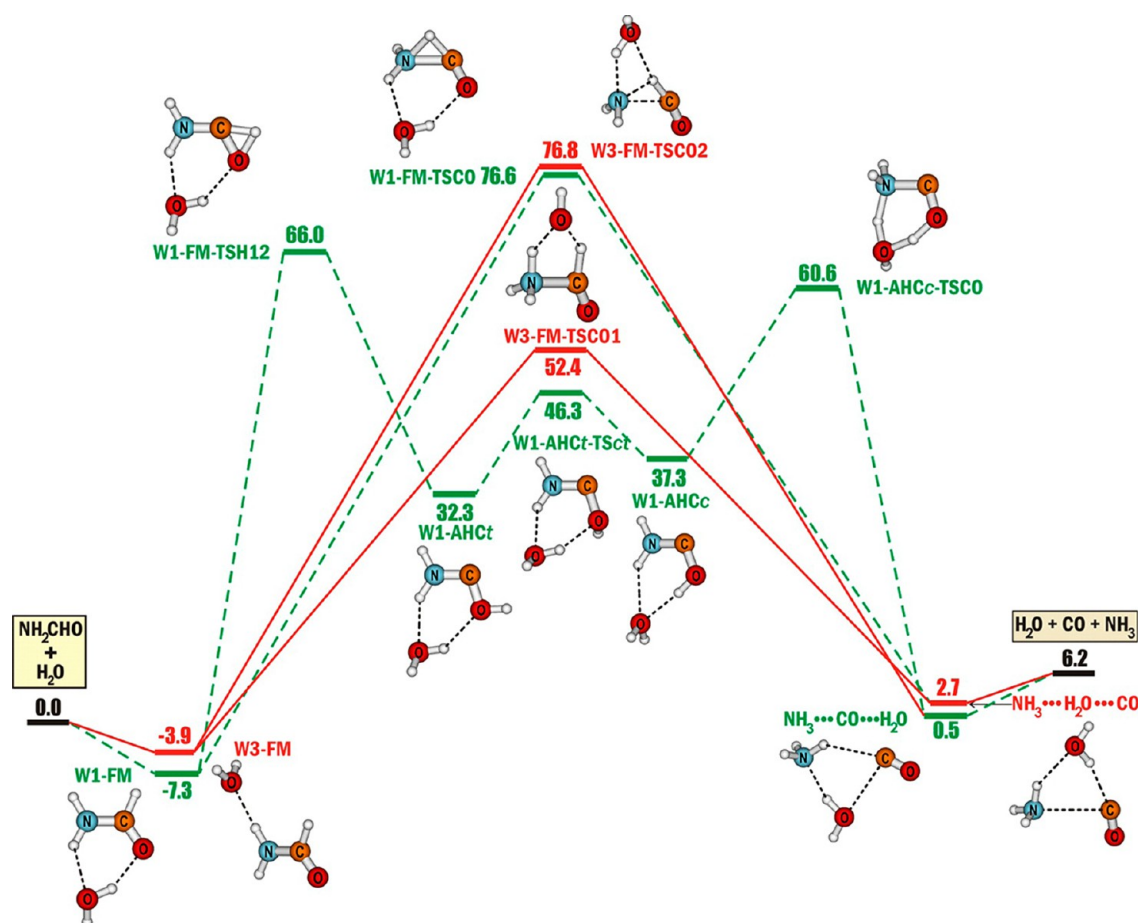


Figure 6. Decarbonylation pathways from complexes **W1-FM** and **W2-FM**. Relative energies in kcal/mol are obtained from CCSD(T)/CBS + ZPE computations.

complex between the TS for 1,2-H-shift of free FM and water at the migrating hydrogen, the latter (at 41.8 kcal/mol) represents a TS in which water plays the role of a bifunctional catalyst. The water molecule classically helps the hydrogen transfer relay within a five-membered cycle (cf. structure of **W2-FM-TSH234** in Figure 7). The substantial difference of about 27 kcal/mol between the energies of both TSs provides a quantitative estimate for a bifunctional catalytic effect exerted on the 1,3-H shift which is an inherently difficult unimolecular rearrangement. In the latter TS, the C–H bond is basically broken while the O–H bond of the carbene is virtually formed. Thus, involvement of just one water molecule strongly improves generation of the higher energy carbene isomer, making it competitive against imine formation (Figure 3). A direct carbene–imine interconversion is also possible but still requires much activation energy via **W2-AHCt-TS1c2a** (at 77.1 kcal/mol).

Proceeding from the most stable complex, isomerizations occur following a reversed pattern. The **W1-FM**–imine **W1-FIA1a** rearrangement becomes markedly facilitated by water-assisted hydrogen transfer, whereas the **FM**–carbene **W1-AHCt** interconversion is stabilized upon H-bonded complexation. The location of the TSs **W1-FM-TS143** at 12.6 kcal/mol for the former process and **W1-FM-TS12** at 66.0 kcal/mol for the latter clearly points out the preferential channel (Figure 5).

Similarly, a comparison of the energy of the TSs for the 1,3-H-shift in free FM (43.9 kcal/mol, Table 2), **W1-FM-TS143** (12.6 kcal/mol, Figure 4), and **W2-FM-TSH13** (39.5 kcal/mol, Figure 2, with respect to the same reference) again demonstrates the

efficiency of acid–base bifunctional catalysis operative in **W1-FM**.

In summary, in interacting with one water molecule, the energy differences between formamide, formalimine, and aminohydroxycarbene isomers are only moderately affected (up to 3 kcal/mol, Table 2), but their interconversions are greatly facilitated by substantial reductions of barrier heights, namely, to 31.3 and 26.9 kcal/mol for **FM**–imine and **FM**–carbene isomerizations, respectively, through water assistance in two distinct approaches.³⁶ With an energy barrier of about 20 kcal/mol, the **W1-FM**–**W1-FIA1a** (imine) rearrangement is expected to occur under mild conditions, and thereby involvement of an imine isomer in **FM** chemistry becomes more likely.

3.2.2. Assisted Dehydration: Reaction 1 with $n = 1$. It turns out that both the H-bonded interaction and bifunctional catalysis equally emerge for this process. We first consider water eliminations arising from the less stable complex, followed then by those involving the most stable one.

A few significant observations can be noted from the calculated results in Figures 3 and 4.

- Dehydration of **FM** is still a multistep process involving either an imine or a carbene conformer. From **W2-FM** the paths giving **HCN** become consistently less favored than those yielding the less stable isomer **HNC** (Figure 3).
- Figure 3 also indicates that dehydration from carbene exhibits a larger energy barrier than those from imine. The lowest energy TS for **HNC** elimination from the lowest energy imine conformer **W2-FIA1a-TSHNC** (see shape

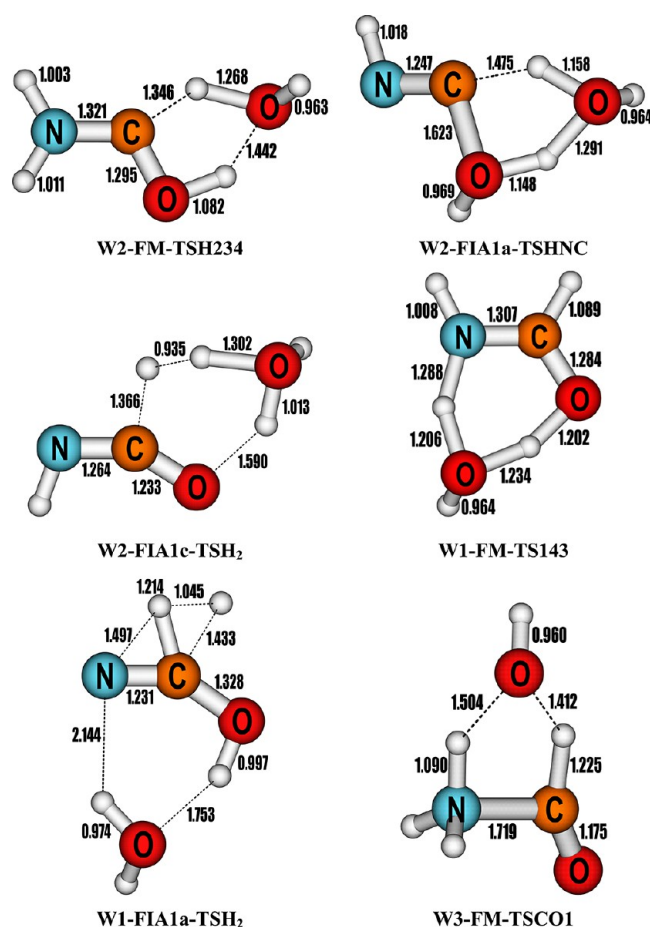


Figure 7. Shape of typical TSs involved in H transfers assisted by one water molecule. MP2/aug-cc-pVTZ bond distances are given in Angstroms.

- in Figure 7) corresponds, in fact, to that for insertion of the HNC carbon end into an O–H framework of the water dimer. Such a TS was previously reported,⁴⁶ and the resulting reduction on barrier height of about 17 kcal/mol with respect to that of free FM (Figure 1) is less important than the amounts mentioned above for other processes. The HCN loss through **W2-FIA1c-TSHCN** (at 69.0 kcal/mol, Figure 3) remains possible but is hardly competitive.
- (iii) From **W1-FM**, dehydration takes place along two main channels. Similar to the W2 case, the first channel passes through a carbene complex **W1-AHCt** producing HNC (Figure 4). Although the associated energy barrier via **W1-AHCt-TSHNC** (63.9 kcal/mol) remains large, due to the high energy of the isomer, it becomes competitive with the **W2-FM** paths mentioned above.
 - (iv) The second channel for H₂O loss implies on its way many imine conformers to end up at **W1-FIA1c-TSHCN**, which is now located at 49.4 kcal/mol (Figure 4). This constitutes the lowest energy point for this multistep transformation and brings about an improvement of 24.2 kcal/mol on the barrier height with respect to that of free FM (73.6 kcal/mol, Figure 1). Such a large amount represents a quantitative effect on FM dehydration induced by the assistance of one water molecule.

3.2.3. Assisted Dehydrogenation: Reaction 2 with $n = 1$. The pathways that we can identify for this reaction mode are schematically illustrated in Figure 5, where critical points

initiated from **W1**, **W2**, and **W3** complexes can be compared to each other.

A process involving **W3-FM** actually concerns dehydrogenation. While H₂ loss is a single-step process from **W3-FM** implying **W3-FM-TSH₂** (61.4 kcal/mol, Figure 5), it follows a multistep path from either **W1-FM** or **W2-FM**. The latter pass through the highest energy TSs **W2-FIA1c-TSH₂** (67.3 kcal/mol) and **W1-FIA1a-TSH₂** (54.9 kcal/mol), respectively, whose shapes are displayed in Figure 7. Thus, H₂ loss from **W3-FM** is associated with a lower barrier height than that within the **W2** series. However, the channel starting from **W1-FM** is found to be the most favored one. Compared to the energy barrier of 78.8 kcal/mol computed for direct H₂ loss from monomeric FM (Figure 1), a water thus induces a reduction of 23.9 kcal/mol, representing a similar order of magnitude with that mentioned above for dehydration.

3.2.4. Assisted Decarbonylation: Reaction 3 with $n = 1$. For this decomposition we are not able to find a relevant pathway initiated from **W2-FM**. The pathways starting from **W1** and **W3** complexes are gathered in Figure 6. Each path leads to two distinct CO-loss channels. The single-step paths going through **W1-FM-TSCO** (76.6 kcal/mol) and **W3-FM-TSCO2** (76.8 kcal/mol) are obviously not competitive due to the large energy barriers. The multistep path from **W1-FM** implying carbene intermediate **W1-AHC** is possible but likely not operative, equally due to the barrier height (at 66.0 kcal/mol) for the preliminary isomerization.

The TS associated with the single step going from **W3-FM** exhibits a specific feature. Its shape displayed in Figure 7 suggests that the water molecule in the complex sharply rotates before transferring an H atom to the N center and subsequently generating a cyclic form by H bonding also with the H(C) atom. The resulting TS **W3-FM-TSCO1** thus resembles an ion pair composed of a protonated formamide and the hydroxy anion (NH₃CHO⁺·OH[−]). The water molecule is regenerated upon formation of CO and NH₃ products. The latter TS, located at 52.4 kcal/mol, turns out to be the most favored for CO elimination under participation of one water molecule (Figure 6).

3.2.5. Preferential Assisted Pathways. Having examined separately the three possible water-assisted decomposition processes, we now can compare their energetics and understand the role of each complex. The main merit of **W2-FM** lies in generation of the high-energy carbene isomer. However, its contributions to FM fragmentations are quite limited due to the large energy barriers, namely, 65.5 and 67.3 kcal/mol for H₂O loss and H₂ elimination, respectively. Dehydrogenation can best be initiated from **W1-FM** passing through a TS located at 54.9 kcal/mol.

In spite of its lower stability, **W3-FM** possesses a suitable conformation for CO production overcoming an energy barrier of 52.4 kcal/mol. The latter is about 3.0 kcal/mol higher than that of 49.4 kcal/mol characterizing the H₂O loss from the most stable **W1-FM**. Considering the expected accuracy of the computational methods employed for the heats of formation, namely, ± 1.0 kcal/mol,^{38,47} the calculated difference of 3.0 kcal/mol lies just outside the error margins. Thus, if the reaction of formamide and one water molecule could take place under appropriate thermodynamic conditions, both dehydration and decarbonylation can be regarded as plausible processes, with an ultimate preference for dehydration. In both channels, the water molecule plays the role of a coreactant and an acid–base

bifunctional catalyst accelerating the H-atom transfer movement within cyclic transition structures.

3.3. Effect of Two Water Molecules on FM Dehydration ($n = 2$). Due to the large number of possible preassociation complexes between FM and two water molecules, we limit our search only to the pathways connecting the most stable trimer. This complex actually corresponds to a W1 type of complex and is thus labeled as **2W1-FM**. Its shape is presented in Figure 8. On

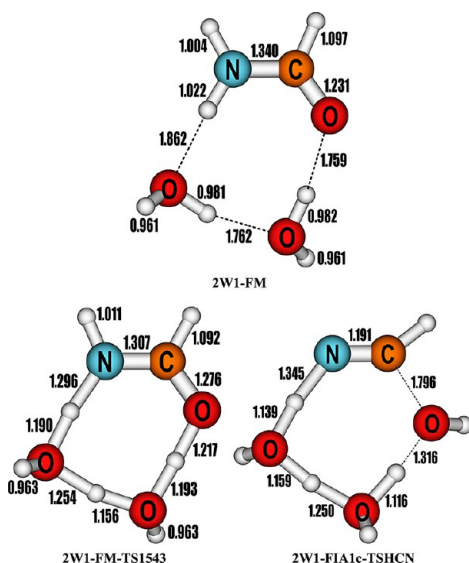


Figure 8. Shape of structures involved in H transfers assisted by two water molecules. MP2/aug-cc-pVTZ bond distances are given in Angstroms.

one hand, in view of the fact that dehydrogenation is characterized with higher energy barriers either without or with

one water molecule, we do not consider it further. On the other hand, we are not able to locate a significant pathway for decarbonylation. The energy profile showing the low-energy pathways for isomerization and dehydration of **2W1-FM** is schematically plotted in Figure 9.

The trimer **2W1-FM** is basically an eight-membered ring containing FM and a water dimer in which three H bonds can be counted. Its binding energy with respect to the separate FM + 2W monomers amounts to 16.2 kcal/mol. The dimerization energy of water was previously determined at 5.0 kcal/mol relative to two monomers (at the same level).³⁸ Accordingly, the binding energy of FM with the water dimer within **2W1-FM** is estimated to be 11.2 kcal/mol, which is substantial. The second water is known to enhance stabilizing interactions with another substrate through a cooperative effect which is mutually polarizing spatially well-aligned H bonds. A similar amount of stabilization can also be found in the trimer of the imine **2W1-FIA1a** (Figure 9).

The second water also acts as a catalyst in rapidly achieving the FM–imine isomerization. Water-assisted conversion of FM proceeding from **2W1-FM** becomes extremely favored with an energy barrier as low as 17.2 kcal/mol via **2W1-FM-TS1543** (located at 1.0 kcal/mol on the energy scale). The latter TS constitutes an extremely compact eight-membered ring in which all X–H bonds are about halfway from their breaking and forming (cf. Figure 8).

Although the imine conformer **2W1-FIA1a** is calculated to be 12.1 kcal/mol less stable than its isomer **2W1-FIA1c**, it again possesses an appropriate geometric configuration for elimination of water within the cyclic **2W1-FIA1c-TS1543** (Figure 8). This TS point is located at 38.0 kcal/mol on the energy profile (Figure 9). Such an energy barrier for dehydration is further reduced as compared to the values of 73.6 and 49.4 kcal/mol obtained without and with one water molecule discussed in previous

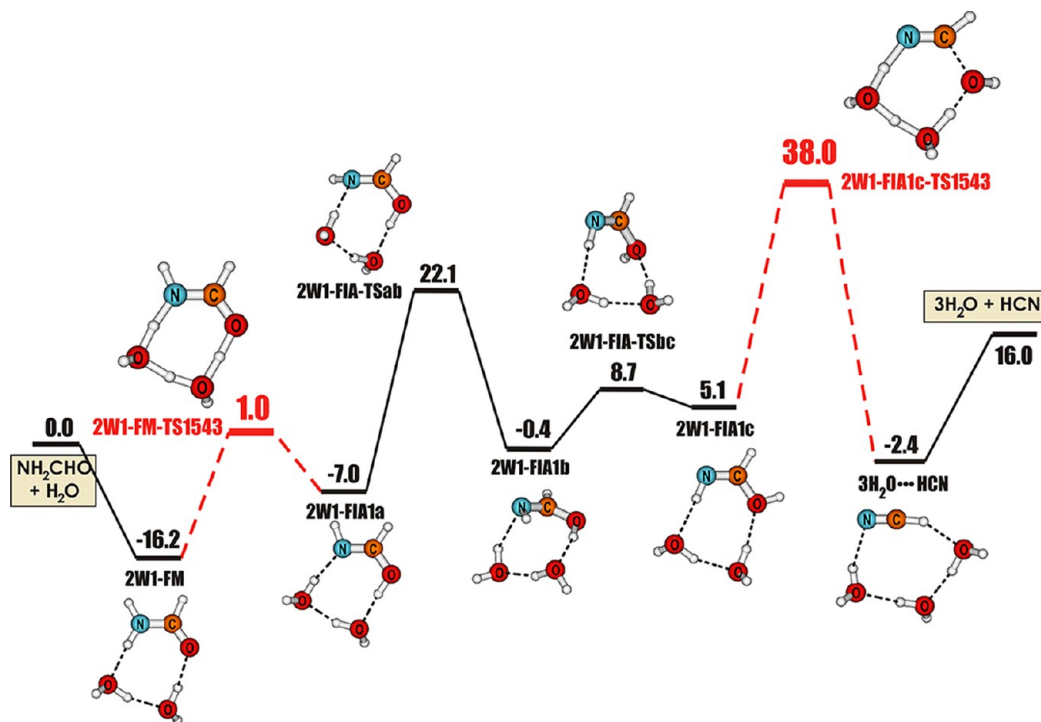


Figure 9. Schematic energy profile illustrating the FM dehydration with the assistance of two water molecules. Relative energies in kcal/mol are obtained from CCSD(T)/CBS + ZPE computations.

sections. In other words, H transfer is further facilitated by the assistance of an additional water molecule.

3.4. Effect of Three Water Molecules on FM Dehydration ($n = 3$). In this section, we again limit our investigation on FM dehydration with the presence of three water molecules. Addition of one extra water molecule tends to enormously increase the actual number of preassociative complexes. Although we explore a number of possible pathways for FM dehydration with the presence of three water molecules, we consider in detail two limiting cases. In the first, we search for complexes formed by interaction of FM and water trimer. In the second case, we take the complex 2W1-FM described above for containing FM + 2W and then place the third water around it in locating stable H-bonded structures. Complex 3W1-FM shown in Figure 10 emerges as the most stabilized tetramer. This

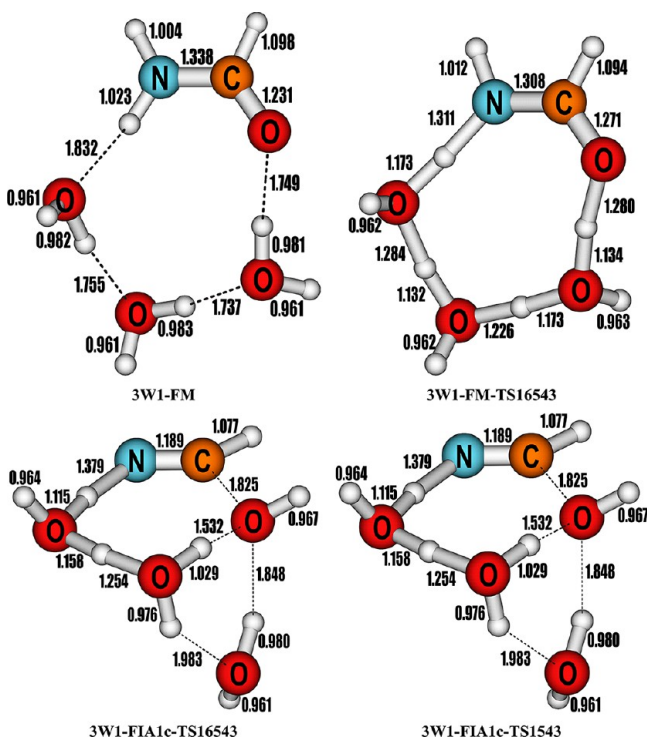


Figure 10. Shape of structures involved in H transfers assisted by three water molecules. MP2/aug-cc-pVDZ bond distances are given in Angstroms.

corresponds to a cyclic complex connecting FM and a water trimer. The alternative complexes 2W1-FM + W are a few kcal/mol less stable. It appears that there are a plethora of possible preassociation complexes and thereby transition structures that differ from each other mainly by the interacting position of the third water molecule. We explore a number of other possible preassociation complexes and transition states of FM dehydration. Most additional preassociation complexes found are however less stable (3.7–5.3 kcal/mol compared to 3W1-FM, obtained at MP2/aVTZ level of theory), and transition structures are characterized by higher energy barriers (located at 62–72 kcal/mol). Some representative complexes and transition structures for water elimination are given in Table S8, Supporting Information. It thus seems reasonable to admit that other complexes are of comparable energies due to the similarity of resulting H-bonded interactions and do not significantly affect the dehydration pattern.

To simplify the presentation of data, we show only for this system the reaction paths related to the most stable complex 3W1-FM that also correspond to the lowest energy barriers. The schematic energy profiles describing the mediated isomerization and dehydration are displayed in Figure 11. Note that the relative energies obtained for this system are evaluated only at the CCSD(T)/aug-cc-pVTZ + ZPE level, and therefore, they cannot directly be compared with the CCSD(T)/CBS values obtained above for smaller systems. However, as demonstrated in section 3.1, they should be quite close to their more accurate CBS counterparts. Deviations are expected to be at most ± 1.5 kcal/mol.

A few important findings can be pointed out from the energy profile of Figure 11.

- With three water molecules involved, the prereaction complex 3W1-FM is further stabilized, which is now situated at 22.6 kcal/mol below the separate monomers. Compared to 2W1-FM, incorporation of the third water brings about an extra stabilization of 6 kcal/mol, which remains significant but somewhat less important than the effect due to interaction of the second water (8.8 kcal/mol). The relative position of the FM–imine isomer pair is not really modified. The most remarkable finding concerning their interconversion is that the relevant 3W1-FM-TS16543 now located at -1.8 kcal/mol on the energy scale. It is thus energetically pushed down to below the monomers asymptote (Figure 11). Nevertheless, due to the stronger stabilization of the FM complex, the energy barrier from the latter tends to increase, as compared to the corresponding situation found in 2W1-FM (Figure 9).
- Formation of HCN also follows a similar route as those with one and two water molecules. The less stable isomer 3W1-FIA1c occupies again a pivotal position as it properly dehydrates FM.
- Two lower lying TSs for water loss are found, and their shape is shown in Figure 10. They have similar energy content, but their geometries markedly differ from each other. The first TS 3W1-FIA1c-TS16543 (at 32.4 kcal/mol) basically describes a relay of H transfer involving all three water molecules (being in fact a trimer 3W). Proceeding in the opposite direction, this TS corresponds to addition of HCN to four water molecules (a tetramer 4W) that fully participate in the cyclic movement of H migration. On the contrary, the TS 3W1-FIA1c-TS1543 (at 31.3 kcal/mol) is actually composed of 2W1-FIA1c-TS1543 of the smaller 2W system described in a previous section, interacting with the third loose water molecule (2W + W). The latter does not participate in the cyclic bond reorganization but interacts further with the more compact TS through microsolvation. Both TSs exhibit comparable energy content with a marginal preference for the 2W + W over the 3W approach. In any case, such barrier heights result from additional stabilization of the relevant TSs.
- The products of both dehydration channels are also similar in energy. While the system 4H₂O-HCN1 seen in Figure 12 involves complexation of HCN with a water tetramer, 4H₂O-HCN2 is basically a complex of HCN with a water trimer plus a separated water monomer.
- These findings suggest that no extra advantage is obtained in terms of activation energies by incorporating more water molecules into the reacting supersystem. Incorporation

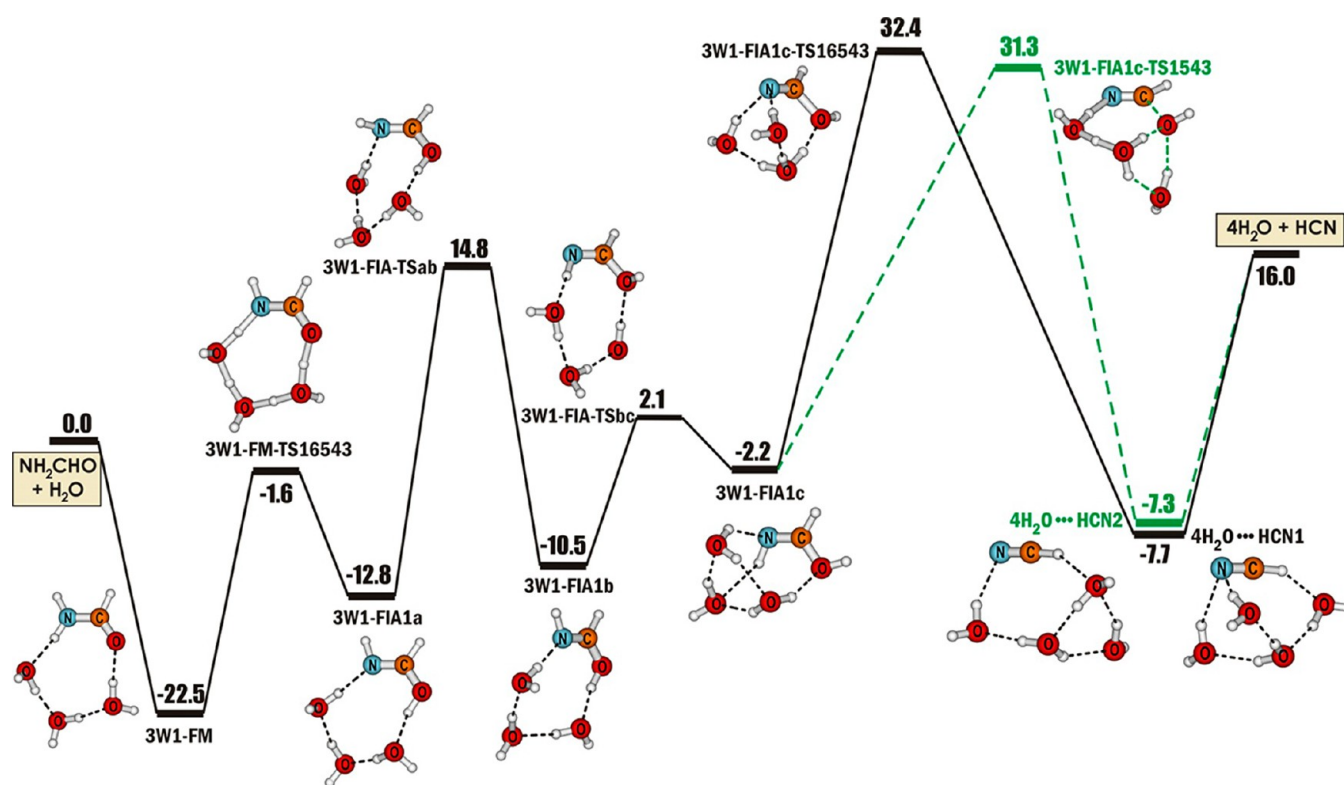


Figure 11. Schematic energy profile illustrating the FM dehydration with the assistance of three water molecules. Relative energies in kcal/mol are obtained from CCSD(T)/aug-cc-pVTZ + ZPE computations.

ration of two active water molecules appears sufficient for the supersystem to integrate the strongest bifunctional catalytic effect. The rest of the water action occurs by microsolvation through multiple H-bonded interactions. Addition of more waters around the stationary points tends to reduce further the barriers, but the resulting stabilizations are relatively small, due to a mutual cancellation of the effects on both the prereaction complexes and TSs.

3.5. Charge Distribution in Transition Structures. In an attempt to probe the electronic mechanism of the water-mediated decomposition of FM, we analyze the topology of the electron densities of some representative transition structures using the atoms in molecules (AIM)⁴⁸ and electron localization function (ELF)⁴⁹ techniques. These consist of a partition of the molecular total density into local basins where electron pairs are concentrated and identified. Both AIM and ELF calculations are carried out using density functional theory with the hybrid B3LYP functional and the aug-cc-pVTZ basis set to generate electron densities. The graphs of bond critical points (BCP) and ELF maps of basins are displayed in Figure 12. In each TS, two BCPs appear around each migrating H atom, which is in addition identified by a basin. The bonds around a migrating H atom have similar bond orders (at the BCP). The similarity of these bond orders indicates a high degree of concertedness of breaking and forming bonds. Each migrating H atom also bears a large positive charge (>0.5 electron) in such a way that it moves, as expected, as a proton between two heavy atom centers bearing large negative charges. Basins covering large domains are localized around the CH bond and O atoms.

A peculiar feature of the AIM graphs shown in Figure 12 is that a ring critical point (RCP) characterizing a cyclic structure does not appear in any TS. This differs from the situation of the

system, such as hydration of carbon dioxide $\text{CO}_2 + (\text{H}_2\text{O})_2$ ³⁸ in which a characteristic RCP emerges in each TS. This suggests a less compact framework of the TSs involving FM and water.

4. CONCLUDING REMARKS

Using ab initio electronic structure calculations, we determined the energetics and molecular mechanisms of the dehydrogenation, decarbonylation, and dehydration of formamide in the presence of small water oligomers in the gas phase. Water classically acts as coreactant and catalyst whose acid–base bifunctional action greatly facilitates the H-transfer relays. Assisted dehydration leading to HCN remains a multistep process and appears to be energetically favored over formation of HNC. Other fragmentation processes are found to be less competitive.

In general, the energy barrier for dehydration of FM decreases with an increasing presence of water molecules. The barrier is thus reduced from 74 kcal/mol in free unimolecular FM to 49, 38, and then 31 kcal/mol, which are due to the active participation of one, two, and three water molecules in the reacting supersystems, respectively. The configuration of the most efficient HCN formation corresponds to a five-membered ring in the transition structure for an imine isomer with one water molecule. Incorporation of extra water molecules (beyond $n = 3$) in the supersystem does not appear to be necessary to facilitate further decomposition.

The calculated energy barriers of ~30 kcal/mol in the presence of water molecules point out that HCN formation from formamide could be achieved under mild thermal conditions. Thus, the present work suggests that one of the possible starting paths from formamide in the long processes forming the nucleobases and other biologically relevant molecules is its initial dehydration.

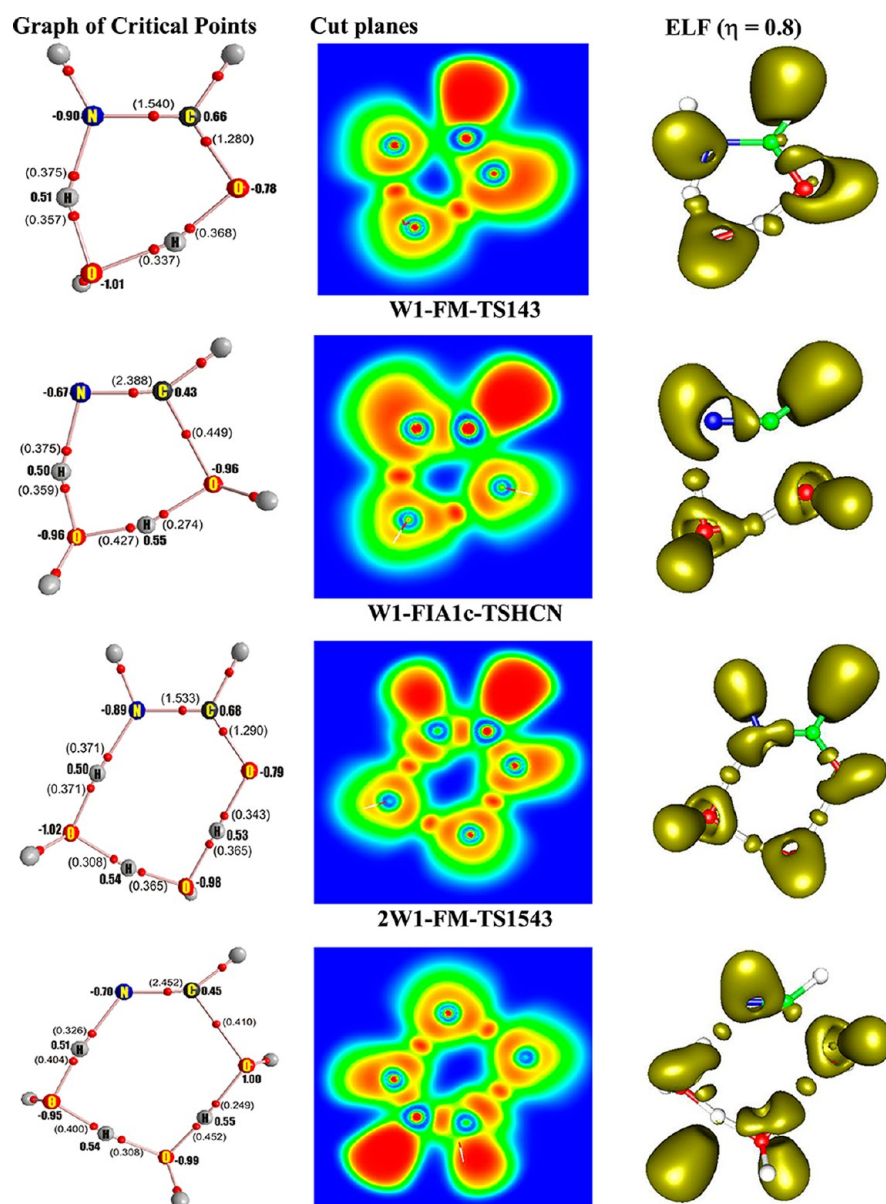


Figure 12. Analysis of the electronic distribution in the transition structures involving one, two, and three water molecules with formamide.

■ ASSOCIATED CONTENT

■ Supporting Information

Figures and Cartesian coordinates of optimized geometries of the structures considered. This material is available free of charge via the Internet at <http://pubs.acs.org>.

■ AUTHOR INFORMATION

Corresponding Author

*E-mail: minh.nguyen@chem.kuleuven.be.

Notes

The authors declare no competing financial interest.

■ ACKNOWLEDGMENTS

The Leuven group is indebted to the KU Leuven Research Council for continuing support through the GOA and IDO programs. T.M.O. and J.L. gratefully acknowledge support from the NSF-NASA Center for Chemical Evolution at Georgia Tech, Atlanta.

■ REFERENCES

- (1) Millar, T. J. *Astrobiology: Future Perspectives*; Kluwer/Springer: Dordrecht, 2004; Chapter 2, p 17 and references therein.
- (2) Markwick, A. J.; Charnley, S. B. *Astrobiology: Future Perspectives*; Kluwer/Springer: Dordrecht, 2004; Chapter 3, p 33–66, and references therein.
- (3) Crovisier, J. *Astrobiology: Future Perspectives*; Kluwer/Springer: Dordrecht, 2004; Chapter 8, p 179–203 and references therein.
- (4) Oparin, A. I. *The Origin of Life*; Macmillan: New York, 1938.
- (5) Miller, S. L. *Science* **1953**, *117*, 528.
- (6) Eschenmoser, A.; Loewenthal, E. *Chem. Soc. Rev.* **1992**, *21*, 1.
- (7) Costanzo, G.; Saladino, R.; Crestini, C.; Ciciriello, F.; Di Mauro, E. *BMC Evol. Biol.* **2007**, *7*, No. S1.
- (8) Gibb, E. L.; Whittet, D. C. B.; Schutte, W. A.; Boogert, A. C. A.; Chiar, J. E.; Ehrenfreund, P.; Gerakines, P. A.; Keane, J. V.; Tielens, A.; van Dishoeck, E. F.; Kerkhof, O. *Astrophys. J.* **2000**, *536*, 347.
- (9) Bockele-Morvan, D.; Lis, D. C.; Wink, J. E.; Despois, D.; Crovisier, J.; Bachiller, R.; Benford, D. J.; Biver, N.; Colom, P.; Davies, J. K.; Gerard, E.; Germain, B.; Houde, M.; Mehringer, D.; Moreno, R.; Paubert, G.; Phillips, T. G.; Rauer, H. *Astron. Astrophys.* **2000**, *353*, 1101.

- (10) Schutte, W. A.; Boogert, A. C. A.; Tielens, A. G. G. M.; Whittet, D. C. B.; Gerakines, P. A.; Chiar, J. E.; Ehrenfreund, P.; Greenberg, J. M.; van Dishoeck, E. F.; de Graauw, T. *Astron. Astrophys.* **1999**, 343, 966.
- (11) Raunier, S.; Chiavassa, T.; Duvernay, F.; Borget, F.; Aycard, J. P.; Dartois, E.; d'Hendecourt, L. *Astron. Astrophys.* **2004**, 416, 165.
- (12) Orgel, L. E. *Crit. Rev. Biochem. Mol. Biol.* **2004**, 39, 99.
- (13) Oró, J. *Biochim. Biophys. Res. Commun.* **1960**, 2, 407.
- (14) Oró, J. *Nature* **1961**, 191, 1193.
- (15) Saladino, R.; Crestini, C.; Ciciriello, F.; Costanzo, G.; Di Mauro, E. *Chem. Biodivers.* **2007**, 4, 694.
- (16) Nguyen, V. S.; Abbott, H. L.; Dawley, M. M.; Orlando, T. M.; Leszczynski, J.; Nguyen, M. T. *J. Phys. Chem. A* **2011**, 115, 841.
- (17) Hudson, J. S.; Eberle, J. F.; Vachhani, R. H.; Rogers, L. C.; Wade, J. H.; Krisnamurthy, R.; Springsteen, G. *Angew. Chem., Int. Ed.* **2012**, 51, 5134.
- (18) Kim, Y.; Lim, S.; Kim, H.-J.; Kim, Y. *J. Phys. Chem. A* **1999**, 103, 617.
- (19) Bakowies, D.; Kollman, P. A. *J. Am. Chem. Soc.* **1999**, 121, 5712.
- (20) Besley, N. A.; Hirst, J. D. *J. Am. Chem. Soc.* **1999**, 121, 8559.
- (21) Garde, S. R.; Kulkarni, A. D. *Indian J. Chem.* **2000**, 39A, 50.
- (22) Chaudhuri, C.; Jiang, J. C.; Wu, C.-C.; Wang, X.; Chang, H.-C. *J. Phys. Chem. A* **2001**, 105, 8906.
- (23) Rest, G. V. D.; Mourgues, P.; Nedev, H.; Audier, H. E. *J. Am. Chem. Soc.* **2002**, 124, 5561.
- (24) Fu, A.-P.; Li, H.-L.; Du, D.-M.; Zhou, Z.-Y. *Chem. Phys. Lett.* **2003**, 382, 332.
- (25) Cascella, M.; Raugei, S.; Carloni, P. *J. Phys. Chem. B* **2004**, 108, 369.
- (26) Liang, W.; Li, H.; Hu, X.; Han, S. *J. Phys. Chem. A* **2004**, 108, 10219.
- (27) Blanco, S.; López, J. C.; Lesarri, A.; Alonso, J. L. *J. Am. Chem. Soc.* **2006**, 128, 12111.
- (28) Almerindo, G. I.; Pliego, J. R. *J. Braz. Chem. Soc.* **2007**, 18 (4), 696.
- (29) Liu, T.; Li, H.; Huang, M.-B.; Duan, Y.; Wang, Z.-X. *J. Phys. Chem. A* **2008**, 112, 5436.
- (30) Bene, J. E. D.; Alkorta, I.; Elguero, J. *J. Phys. Chem. A* **2008**, 112, 6338.
- (31) Sakai, D.; Matsuda, Y.; Hachiya, M.; Mori, M.; Fujii, A.; Mikami, N. *J. Phys. Chem. A* **2008**, 112, 6840.
- (32) Maeda, S.; Matsuda, Y.; Mizutano, S.; Fujii, A.; Ohno, K. *J. Phys. Chem. A* **2010**, 114, 11896.
- (33) Angelina, E. L.; Peruchena, N. M. *J. Phys. Chem. A* **2011**, 115, 4701.
- (34) Mahadevi, A. S.; Neela, Y. I.; Sastry, G. N. *Phys. Chem. Chem. Phys.* **2011**, 13, 15211.
- (35) Mahadevi, A. S.; Neela, Y. I.; Sastry, G. N. *J. Chem. Sci.* **2012**, 1, 35.
- (36) (a) Nguyen, M. T.; Ha, T. K. *J. Am. Chem. Soc.* **1984**, 106, 599. (b) Nguyen, M. T.; Raspoet, G.; Vanquickenborne, L. G.; Van Duijnen, P. Th. *J. Phys. Chem. A* **1997**, 101, 7379.
- (37) Lewis, M.; Glaser, R. *J. Phys. Chem. A* **2003**, 107, 6814.
- (38) Nguyen, M. T.; Matus, M. H.; Jackson, V. E.; Ngan, V. T.; Rustad, J. R.; Dixon, D. A. *J. Phys. Chem. A* **2008**, 112, 10386.
- (39) Frisch, M. J.; Trucks, G. W.; Schlegel, H. B.; Scuseria, G. E.; Robb, M. A.; Cheeseman, J. R.; Montgomery, J. A., Jr.; Vreven, T.; Kudin, K. N. et al. *Gaussian 03*; Gaussian: Wallingford, CT, 2004.
- (40) Knowles, H.-J. W. P. J.; Amos, R. D.; Bernhardsson, A.; Berning, A.; Celani, P.; Cooper, D. L.; Deegan, M. J. O.; Dobbyn, A. J.; Eckert, F.; Hampel, C.; Hetzer, G.; Korona, T.; Lindh, R.; Lloyd, A. W.; McNicholas, S. J.; Manby, F. R.; Meyer, W.; Mura, M. E.; Nicklass, A.; Palmieri, P.; Pitzer, R. M.; Rauhut, G.; Schutz, M.; Stoll, H.; Stone, A. J.; Tarroni, R.; Thorsteinsson, T. *MOLPRO-2002, a package of initio programs*; University of Birmingham and University Stuttgart: Birmingham, U.K., and Stuttgart, Germany, 2002.
- (41) Cizek, J. *Adv. Chem. Phys.* **1969**, 14, 35.
- (42) Raghavachari, K.; Trucks, G. W.; Pople, J. A.; Head-Gordon, M. *Chem. Phys. Lett.* **1989**, 157, 479.
- (43) Dunning, T. H. *J. Chem. Phys.* **1989**, 90, 1007.
- (44) Kendall, R. A.; Dunning, T. H.; Harrison, R. J. *J. Chem. Phys.* **1992**, 96, 6796.
- (45) Peterson, K. A.; Woon, D. E.; Dunning, T. H. *J. Chem. Phys.* **1994**, 100, 7410.
- (46) Nguyen, M. T.; Hegarty, A. F. *J. Chem. Soc., Perkin Trans. 2* **1987**, 1675.
- (47) (a) Matus, M. H.; Nguyen, M. T.; Dixon, D. A. *J. Phys. Chem A* **2006**, 110, 8864. (b) Nguyen, M. T.; Matus, M. H.; Ngan, V. T.; Haiges, R.; Christie, K. O.; Dixon, D. A. *J. Phys. Chem. A* **2008**, 112, 1218. (c) Nguyen, M. T.; Nguyen, V. S.; Matus, M. H.; Gopakumar, G.; Dixon, D. A. *J. Phys. Chem A* **2007**, 111, 679.
- (48) Bader, R. F. W. *Atoms in Molecules. A Quantum Theory*; Oxford University Press: New York, 1995.
- (49) Silvi, B.; Savin, A. *Nature* **1994**, 371, 63.